REPORT DOCUMENTATION PAGE

Form Approved
OMB No. 0704-0188

1. REPORT DATE *(DD-MM-YYYY)*	**2. REPORT TYPE**	**3. DATES COVERED** *(From - To)*
13-07-2011	Conference Paper	

4. TITLE AND SUBTITLE

Effect of Swirl on Gas-Centered Swirl-Coaxial Injectors Propulsion Systems

5a. CONTRACT NUMBER

5b. GRANT NUMBER

5c. PROGRAM ELEMENT NUMBER

6. AUTHOR(S)
S.A. Schumaker, S. A. Danczyk, and Malissa D.A. Lightfoot

5d. PROJECT NUMBER

5f. WORK UNIT NUMBER
50260538

7. PERFORMING ORGANIZATION NAME(S) AND ADDRESS(ES)

Air Force Research Laboratory (AFMC)
AFRL/RZSA
10 E. Saturn Blvd.
Edwards AFB CA 93524-7680

8. PERFORMING ORGANIZATION REPORT NUMBER

AFRL-RZ-ED-TP-2011-303

9. SPONSORING / MONITORING AGENCY NAME(S) AND ADDRESS(ES)

Air Force Research Laboratory (AFMC)
AFRL/RZS
5 Pollux Drive
Edwards AFB CA 93524-7048

10. SPONSOR/MONITOR'S ACRONYM(S)

11. SPONSOR/MONITOR'S NUMBER(S)
AFRL-RZ-ED-TP-2011-303

12. DISTRIBUTION / AVAILABILITY STATEMENT

Approved for public release; distribution unlimited (PA #11308).

13. SUPPLEMENTARY NOTES
For presentation at the 47th AIAA Joint Propulsion Conference, to be held in San Diego, CA, 31 Jul - 3 Aug 2011.

14. ABSTRACT

Physics-based scaling laws and design methodologies for gas-centered swirl-coaxial injectors have been under consideration for several years. Prior work showed that scaling via a momentum flux ratio was promising. However, that work neglected the effects of liquid swirl on the atomization. This current work refines the definition of the momentum flux ratio by adding compressibility in the gas phase and using a total liquid velocity. The focus, however, is on the impact of swirl through the study of different liquid inlet configurations. The film length and character are studied for a range of swirl values with ratios of axial to total velocity ranging from 26 to 41 percent. The new definition of momentum flux ratio collapses film length data onto a single curve over the range of swirl levels and interior injector geometries. The character of the film is seen to change, particularly in regards to gas entrainment into the film, as the swirl is decreased. Changes in swirl have little impact on film length; this is anticipated because the centripetal forces are several orders of magnitude lower than the aerodynamic forces driving atomization. Some examination of an inlet with no swirl (axial to total velocity ratio of 100 percent) is also presented.

15. SUBJECT TERMS

16. SECURITY CLASSIFICATION OF:			**17. LIMITATION OF ABSTRACT**	**18. NUMBER OF PAGES**	**19a. NAME OF RESPONSIBLE PERSON**
					S.A. Schumaker
a. REPORT	**b. ABSTRACT**	**c. THIS PAGE**	SAR	16	**19b. TELEPHONE NUMBER** *(include area code)*
Unclassified	**Unclassified**	**Unclassified**			N/A

Effect of Swirl on Gas-Centered Swirl-Coaxial Injectors

S. Alexander Schumaker[1], Stephen A. Danczyk[2] and Malissa D.A. Lightfoot[3]
Air Force Research Laboratory, Edwards AFB, CA, 93524

Physics-based scaling laws and design methodologies for gas-centered swirl-coaxial injectors have been under consideration for several years. Prior work showed that scaling via a momentum flux ratio was promising. However, that work neglected the effects of liquid swirl on the atomization. This current work refines the definition of the momentum flux ratio by adding compressibility in the gas phase and using a total liquid velocity. The focus, however, is on the impact of swirl through the study of different liquid inlet configurations. The film length and character are studied for a range of swirl values with ratios of axial to total velocity ranging from 26 to 41 percent. The new definition of momentum flux ratio collapses film length data onto a single curve over the range of swirl levels and interior injector geometries. The character of the film is seen to change, particularly in regards to gas entrainment into the film, as the swirl is decreased. Changes in swirl have little impact on film length; this is anticipated because the centripetal forces are several orders of magnitude lower than the aerodynamic forces driving atomization. Some examination of an inlet with no swirl (axial to total velocity ratio of 100 percent) is also presented.

Nomenclature

A_{surf}	=	Surface area of a disturbance on the film's surface
A^*	=	Calculated throat area
Fr_c	=	PseudoFroude number for centripetal force
L_C	=	Injector cup length
L_f	=	Liquid film length
$\dot{m}$	=	Mass flow rate
R_A	=	Ratio of axial to total film velocity at injector lip
r_g	=	Initial injector gas post radius
r_o	=	Injector outlet radius
r_p	=	Injector gas post radius at end of sheltered lip
Re	=	Reynolds Number
s	=	Injector step height at end of sheltered lip
v	=	Velocity
Vol	=	Volume
We	=	Weber number of the liquid
X	=	Downstream coordinate
Y	=	Radial coordinate
Φ	=	Gas to liquid momentum flux ratio
ρ	=	Density
τ	=	Initial liquid film thickness

Subscripts

axial	=	Denotes axial component of the liquid velocity
dis	=	Of a disturbance on the film's surface
g	=	Denotes a gas property
l	=	Denotes a liquid property
tan	=	Denotes tangential component of the liquid velocity
total	=	Denotes total liquid velocity

[1] Aerospace Engineer, RZSA, 10 E. Saturn Blvd., and Member AIAA.
[2] Research Scientist, RZSA, 10 E. Saturn Blvd., and Member AIAA.
[3] Aerospace Engineer, RZSA, 10 E. Saturn Blvd., and Member AIAA.

I. Introduction

As the rocket community around the world moves to increase performance and decrease launch and development costs more emphasis is being placed on small-scale and single-element studies. The development of scaling laws and design criteria for specific rocket components at the single-element level greatly reduces the time and costs of engine programs. For the injector component, this type of single-element investigation has been carried out for decades. However, most work has focused on specific types of injectors. As engine cycles and operating conditions change, so do the candidate injectors. For much of the past, each time the candidate injector changed, a new test campaign was needed to produce the necessary design methodologies for that particular injector. However, recent work has focused on physics-based understanding that is applicable to a range of injector types while validating the developed methodologies against the specific injector of current interest—a gas-centered swirl coaxial (GCSC) injector.[1, 2]

Gas-centered swirl coaxial injectors, a specific type of prefilming airblast atomizer, have seen an increase in interest over the last decade.[3-6] They have high performance at the flow conditions typical in OX rich staged combustion cycles, especially those involving rocket-grade kerosene (RP). This type of element was also used successfully in Russian rocket engines employing an OX rich staged combustion cycle (eg, RD-170).[7] However, the basic scaling and design criteria were not well documented and physics-based models did not exist. Because the interest, throughout the world, in RP-GOX and gas-generator cycles has been on the increase in recent years,[3-6] much effort has been placed on constructing the needed design and scaling methodologies.

Already, a physics-based scaling law has been developed.[8] It applies to GCSC injectors as well as other injectors where the gas-phase strongly participates in the breakup and mixing of the fuel and oxidizer. The parameter being predicted by this law is ultimately the atomization performance of the injector. Atomization performance can be directly related to mixing efficiency and is predicted, in large part, by a combination of the film length and the gas velocity.[8] Mixing efficiency, in turn, is directly related to engine performance—mixing must occur before the combustion can take place, so increased mixing efficiency means a shorter mixing length and, therefore, a shorter length for complete combustion. The film length is not only important for insuring atomization performance, but it also can have a direct impact on engine lifetime. If the film is longer than the injector then poor atomization performance results because large droplets are created on the periphery of the spray.[9] However, if the film is too short insufficient cooling could cause melting of the injector. Note that combustion is known to occur in the cup of these injectors. The film will also not be present to cool the outlet of the injector. This combination is likely to cause melting or erosion of the injector faceplate reducing engine lifetimes and possibly leading to catastrophic failure in a short time period.

The developed scaling law shows that the momentum flux ratio is the main scaling parameter for atomization efficiency in GCSC injectors.[2] Due to its simplified and general nature, the model does not explicitly specify the calculation of the momentum flux ratio. Indeed, the calculation is not straightforward as there is not a single gas velocity nor is there a single liquid velocity within the injector, and the velocities at the interface are not known. These velocities are difficult and expensive to measure; they could possibly be calculated using CFD but not in a cost-effective or time-effective manner.[3] As a result, it is necessary to develop a formulation of the momentum flux ratio which may be calculated without prior knowledge of the velocities. Such a formulation was developed in an earlier work;[2] however, this work did not consider all of the effects likely to be present in a GCSC injector. A prime limitation was the effect of swirl not being considered.

Swirl impacts the atomization performance of a GCSC injector in two main ways. First, the velocity vector of the liquid is not in line with the velocity vector of the gas. This means that the shear seen by the interface is not based on the difference between the total liquid velocity and gas velocity but on some pro-rated liquid velocity. Secondly, the swirl imparts a centripetal force to the liquid. These two effects and their impact on the scaling and general character of the liquid film and atomization process are the primary focus of this paper. Experimental results from several GCSC injectors with four different inlet geometries are presented. An improvement in the definition of the velocities, which accounts for swirl as well as compressibility of the gas, is added to the momentum flux ratio and compared with the experimental results. Final recommendations on using swirl in the design of injectors are presented.

II. Experimental Setup

Gas-centered swirl-coaxial injectors are a type of air blast atomizer which utilizes an axial, fast-moving gas stream to strip droplets from a swirling, wall bounded film. Unswirled gas enters down the centerline of the injector while the film is created by introducing liquid through holes tangentially drilled into the injector cup. The injector used in

this study is of a modular design that allows the injector geometry to be easily varied. The acrylic main injector body is changeable allowing the outlet radius, along with the diameter and number of liquid inlet holes to be changed. Results are presented with outlet radii of 7.62, 9.53, and 11.4mm. An interchangeable insert, also made of acrylic, forms the bottom part of the gas post and the initial sheltered cup for the liquid which allows for the gas post radii to be varied between 3.43mm and 9.27mm with initial film thicknesses of 1.32, 1.65 and 1.98mm. The upper portion of the gas post is a stainless steel plenum 180mm in length with a fixed radius of 6.25 mm resulting in an inlet L/D ratio of ~14. Depending on the gas post radius at the end of the sheltered lip the last 45.5mm of the gas post can be straight, converging, or diverging. All injectors presented here have a cup length of 33.0mm. Specific injector cup geometries are given in Table 1.

Name	r_o (mm)	τ (mm)	r_p (mm)	s (mm)
ODHNTN	7.620	1.651	4.445	1.524
ONPDTN	9.525	1.651	5.461	2.413
ONPNTN	9.525	1.651	6.350	1.524
ONPUTN	9.525	1.651	7.468	0.406
OUHUTD	11.43	1.321	7.239	2.870

Table 1. The insert names and their attendant geometries are given above. The naming convention is to list the relative size of the (O)utlet and (P)ost radii and the film (T)hickness as either (D)own or (U)p from (N)ominal. In some inserts the (H)eight of the step plus film thickness is referenced instead of the gas post radius.

In an effort to explore the effect of swirl on primary atomization, four injector bodies with varying degrees of swirl were used. The baseline injector body, which has been used in prior studies,[2] has four tangential inlets holes of diameter 1.60mm this arrangement produces an axial to total velocity ratio (R_A) of 30 percent. In the results section this inlet configuration is designated by 4H- followed by the insert nomenclature given in the caption of Table 1. The other three injector bodies use an eight inlet hole configuration. The first eight-hole configuration has the same hole diameter as the four hole case which results in double the liquid inlet flow area producing an R_A value of 41 percent. The double area configuration is designated by 8H-DA-insert. The second eight-hole configuration has approximately the same flow area as the baseline injector but twice the number of holes resulting in inlet hole diameters of 0.989 mm and a R_A of 26 percent. The same area case is designated by 8H-insert. The final eight-hole injector body was designed without swirl. The no swirl injector body (designated by NS-insert) has the same hole diameters as the same area case, but instead of the hole being drilled tangential to the cup the holes were drilled perpendicular to the cup. Sketches of these configurations are shown in Fig. 1. Swirl quantities are given in terms of the axial to total velocity ratios since the swirl number, typically designated by tangential over total velocity, is close to 1 and difficult to distinguish between cases.

When utilized in a staged-combustion-cycle liquid-rocket engine with a liquid-oxygen full-flow preburner the gas like-phase would typically be oxygen and the wall-bounded film would be a kerosene-based fuel. In this cold-flow study, water and gaseous nitrogen are used as surrogates. Gas and liquid flow rates are controlled using calibrated sonic nozzles and cavitating venturis, respectively. The calibration and selected pressure transducers allow mass flow rates to be known to ~0.23 g/s. A valve downstream of the venturi (but upstream of the injector) insures that there is sufficient back pressure to minimize acoustic noise. All tests are performed with atmospheric back pressure. The gas flow rates were varied from 0.004-0.103 kg/s and liquid flow rates were varied from 0.011-0.122 kg/s. Due to pressure drops in the flow system, previous studies observed bubbles in the injector cup from

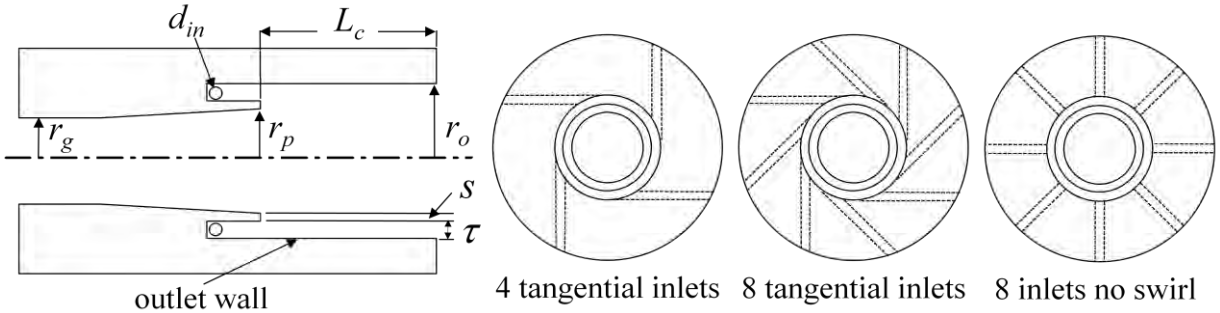

Figure 1. In this schematic of a gas-centered swirl-coaxial injector r_g represents the initial gas radius (always 6.35 mm), L_c the injector cup length (always 33 mm), r_p the gas post radius at the end of the sheltering lip, r_o the outlet radius, S the step height, τ the initial film thickness, and d_{in} the liquid inlet diameter. Three liquid inlet geometries are shown: 4 tangential inlets, 8 tangential inlets, and 8 inlets no swirl. Table 1 lists the values of these dimensions used in the experiments.

dissolved gas coming out of solution upstream of the injector cup. To eliminate these bubbles the water run tank was placed under vacuum for 8-12 hours before testing. A bubble trap was also added downstream of the cavitating venturi to eliminate any remaining bubbles. To aid in the calculation of flow properties in the gas plenum, a static pressure measurement was made 49.1mm upstream of the gas post lip. Also, total temperature measurements were made in the gas and liquid upstream of the sonic nozzle and cavitating venturi, respectively.

Liquid film profiles were imaged using a two-laser lighting method. Two, green, 500 mW, adjustable-power, DPSS lasers were placed on opposite sides of the test section. Identical combinations of cylindrical concave and spherical convex lenses were used with each laser to form a two inch high laser sheet. After aligning the two sheets on top of each other, the acrylic injector body was placed in the middle of the two-laser setup. The sheets were placed 0.5 to 1 mm forward of the injector midline to maximize light scattering to the camera. A schematic of the setup is shown in Fig. 2. A Vision Research Phantom v7.3 camera positioned 90° from the sheets was used to capture the video at 6006 fps. The exposure time was 150 microseconds. The power of each laser was adjusted independently to achieve equal lighting and adequate intensity of both the top and bottom film. Assessment of each setting was performed by eye.

Image processing was done via Matlab routines to obtain average and instantaneous film profiles. Once a 14-bit image was converted to an array, vertical slices of the picture were examined. Each vertical slice was further divided into two areas where the film interface was likely to occur (since the film is visible on both sides of the injector). These windows were based on the known edge of the injector body and the previous maximum location of the film (near the beginning, a maximum possible height based on the distance to the top of the sheltering lip was used). Within these windows the largest continuous increase in intensity was marked as containing the film boundary and the largest increase over a single pixel within this area was chosen as the actual boundary. Lighting variations due to the turbulent nature of the flow and the atomization process occasionally produce difficulties, so care must be taken to ensure bright areas due to these variations are not mistakenly labeled as film boundaries. Final acceptance of the film profile was based on user viewing of the original movies with the found film profiles overlaid. In earlier work insufficient or nonuniform lighting resulted in a nontrivial percentage of movies being unusable.[10] However, the two-laser setup used here largely eliminated these problems. Average film profiles and average lengths were 5000 instantaneous image results averaged together (approximately 1000 more than analysis indicated was needed for the averages to fully converge). Due to the lighting changes and the ever-thinning nature of the film, it is difficult to estimate the accuracy with which the length is actually captured. Additionally, the film length is not steady. The accuracy expected, then, can be based on the standard deviation of the measured film length which is reported later. However, a significant percentage of the standard deviation is real film fluctuations.

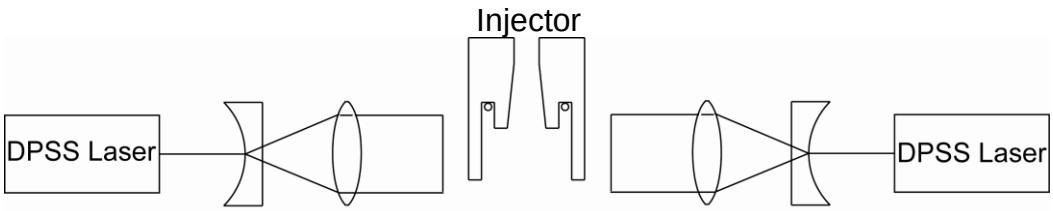

Figure 2. The two-laser experimental setup used to image the wall bounded film profiles. The laser sheets illuminated the test article from just upstream of the sheltered lip to a few mm below the end of the injector.

III. Scaling

Previous studies of the atomization mechanisms have identified three phenomena that cause atomization from wall-bounded films: liquid turbulence, stripping of waves, and stripping/tearing resulting from gas-phase vortices.[11] The relative importance of the forces that drive these mechanisms can be gauged by looking at six nondimensional parameters: momentum flux ratio, Weber number (We), Reynolds number (Re) (both gas and liquid phase), and two pseudoFroude numbers.[1] These nondimensional parameters account for aerodynamic, surface tension, viscous, gravity and centripetal forces, respectively. When used as rocket propellant injectors, GCSC injectors operate in a high Weber number and Reynolds number regime and, therefore, viscous and surface tension effects are small.[1] For example one case with the 8H-ONPNTN geometry and a momentum flux ratio (Φ_{total}) of 114, has a gas phase Reynolds number (Re_g) of 1,000,000 and a Weber number (We) of 44. Table 2 gives a value range for these nondimensional parameters and mass flow rates for each of the fourteen geometries used in this study. In the regime where GSCS injectors operate in liquid rocket engines aerodynamic forces are dominant, but centripetal forces can play a role at lower values of the momentum flux ratio and therefore should not be ignored. If the six

nondimensional parameters are examined it can be shown that the liquid phase viscous forces and centripetal forces are of roughly equal magnitude but both are small compared to the aerodynamic forces and the surface tension, gravity, and gas phase viscous forces are at least one order of magnitude less than the liquid phase viscous and centripetal force. Earlier works have presented arguments that atomization rate is related to a single disturbance is related to the entire film and, therefore, to the film length. From this argument and the nature of the aerodynamic forces it is expected that the film length should be strongly related to the momentum flux ratio and an indicator of overall spray quality (droplet size and distribution).

Difficulties arise when defining the momentum flux ratio in GCSC injectors due to the complex compressible flow fields inside the injector cup. This complex field makes the use of a single velocity to describe the aerodynamic forces acting on the film inaccurate. Also, to be of use in engineering calculations, variables, used to define the scaling parameters, such as velocity, should be easily calculable or measurable. In previous work a number of logical scaling parameters were explored using basic average velocities and the best collapse of available film length data was found using velocities based on the initial film thickness and the average gas-post radius from contact with the film to the exit.[10] Mathematically this resulted in the momentum flux ratio being defined as

$$\Phi_{\text{axial}} = \left(\frac{\rho_l}{\rho_g}\right)\left(\frac{m_g}{m_l}\right)^2 \{\tau(2r_o - \tau)/[r_o - (\tau + s)/2]^2\}^2 \,. \tag{1}$$

This definition is based on the mass flow rates of the liquid and gas because they are the measured quantities. This definition uses only the axial portion of the liquid velocity, ignoring the swirling component. In the past this definition used the gas phase density based on the injector exit pressure, not the static pressure in the gas post. Earlier work with the momentum flux ratio defined in Eq. 1 was able to show that the film length corresponded to the momentum flux ratio; however, this definition of the momentum flux ratio was unable to fully collapse all geometries to a single curve, resulting instead in a family of curves.[10] A new definition was sought to achieve a better collapse.

Returning to the basic definition of the momentum flux ratio,

$$\Phi_{\text{total}} = \left(\frac{\rho_g}{\rho_l}\right)\left(\frac{v_g}{v_l}\right)^2 \,, \tag{2}$$

methods were explored to more accurately capture the complex density and velocity field of the gas phase and the velocity field of the liquid. Since it is impractical to directly measure the velocity at the end of the gas post, velocity and density were calculated using one-dimensional gas dynamics from measured values of the total temperature, mass flow rate and static pressure. Starting at the location of the static pressure port in the gas plenum (49.1mm upstream of the gas post lip) and assuming quasi-one-dimensional flow and a calorically perfect gas, the Mach number can be calculated from the mass flow rate equation. Using perfect gas and the isentropic equations all flow properties at the static pressure port location are easily calculated. Since the injectors used here can have a straight, converging or diverging gas plenum downstream of the static pressure point the conditions at the static pressure point have to be extrapolated to the gas post lip using the area-Mach number relation and the isentropic equations. Mach number at the gas post lip varied from 0.1 to 1.0 with the vast majority of cases clustered between 0.5-0.9. In the cases where the calculated throat area (A^*) was slightly less than or the same as the actual area at the gas post lip, the gas post exit was assumed to be a sonic throat and a Mach number of 1 was used for velocity and density calculations. A sonic condition at the gas post lip occurred in a majority of the cases run with the ONPDTN insert which has a converging gas post.

Due to the swirl component of the liquid velocity vector it is not clear from scaling arguments alone what is the proper choice for the liquid phase velocity. Possibilities include the total velocity (vector addition of the tangential and axial velocity) or the axial velocity (aligned with the injector centerline). After exploring a number of logical options the best fit to the available data was found using the total velocity at the liquid cup exit. The total velocity was calculated by assuming that the momentum of the liquid was conserved between the tangential liquid injector holes and the liquid cup exit. This assumption obviously ignores the losses in the liquid cup. The axial component of velocity was calculated from simple mass flow arguments and the known liquid cup area. For the no swirl cases conservation of momentum was not used and the mass flow rate and liquid cup area was used to calculate the total velocity. Correlations of film length with this definition of the momentum flux ratio for varying level of swirl are presented in Section IV.

While not as strong as the aerodynamic forces on the liquid film, especially at large Φ_{total} values, the centripetal force is expected to play some role in the atomization process especially at lower values of the momentum flux ratio. The centripetal force acts opposite of the aerodynamic forces to stabilize the film by decreasing the size and growth rate of any disturbances caused by aerodynamic forces on the film surface. Through this process entrainment of gas into the liquid film is hindered due to the difference in density between the two fluids and the buoyancy type force created by the centripetal acceleration. The centripetal force represented by a pseudoFroude number (Fr_c) is related

to the ratio of tangential to total velocities. As mentioned earlier, this is near unity. The other term in this pseudoFroude number is the ratio of the disturbance's volume to its surface area. Combing these two terms the pseudoFroude number for centripetal force can be represented by

$$\mathrm{Fr_c} = \left(\frac{v_{radial}}{Vv_{total}}\right)^2 \left(\frac{Vol}{r_o{*}A_{surf}}\right)_{dis} . \quad (3)$$

If the disturbance is assumed to be roughly toroidal, the maximum ratio of the disturbance's volume to its surface area is τ. For a hemi-spherical disturbance this would be $\tau/3$ at maximum (maximum disturbance height is film thickness). Finally, then, the pseudoFroude number is, at most,

$$\mathrm{Fr_c} = \left(\frac{v_{radial}}{v_{total}}\right)^2 \left(\frac{\tau}{r_o}\right) . \quad (4)$$

Values of this pseudoFroude number varied between 0 and 0.195 for the geometries and cases investigated here.

Geometry	$\dot{m}_g$ (g/s)	$\dot{m}_l$ (g/s)	Φ_{total}	R_A	Re_g	Re_l	We	Fr_C
4H-OUHUTD	19-82	24-63	3.1-104	0.286	136,000-490,000	1,250-3,350	15-110	0.108
4H-ONPNTN	23-71	33-68	11-103	0.299	199,000-667,000	2,040-4,230	33-143	0.158
4H-ODHNTN	23-73	37-57	16-100	0.320	377,000-1,300,000	2,750-4,270	61-146	0.195
4H-ONPUTN	25-73	32-65	6.3-43	0.299	167,000-462,000	2,020-4,080	33-133	0.158
4H-ONPDTN	20-70	33-73	11-156	0.299	217,000-971,000	2,080-4,600	34-169	0.158
8H-DA-ONPNTN	32-71	32-84	29-191	0.406	288,000-667,000	1,440-3,900	17-120	0.145
8H-DA-ONPUTN	25-69	24-59	12-111	0.406	179,000-501,000	1,070-2,640	10-59	0.145
8H-DA-ONPDTN	30-67	36-97	29-203	0.406	319,000-770,000	1,600-4,400	22-159	0.145
8H-ONPNTN	48-103	25-51	21-140	0.261	452,000-1,010,000	1,720-3,700	25-109	0.162
8H-ONPUTN	46-92	18-46	12-88	0.261	338,000-686,000	1,260-3,200	13-86	0.162
8H-ONPDTN	58-88	25-65	38-206	0.261	663,000-1,050,000	1,710-4,550	26-174	0.162
8H-NS-ONPNTN	48-103	25-52	21-140	0.261	452,000-1,010,000	1,720-3,690	25-109	0.162
8H-NS-ONPUTN	46-92	18-46	12-88	0.261	338,000-686,000	1,260-3,200	13-86	0.162
8H-NS-ONPDTN	58-88	25-65	38-206	0.261	663,000-1,050,000	1,710-4,550	26-174	0.162

Table 2. Ranges of mass flow rates and nondimensional parameters for the fourteen geometries used in this work.

IV. Results & Discussion

To explore the effect of varying levels of swirl on the film length and profile of GCSC injectors average and instantaneous film profiles were obtained in twelve different injector configurations (four different liquid inlet hole variations and three different injector cup geometries). Over these geometries the axial to total velocity ratio (R_A) is varied between 26 and 100 percent. Understanding the role swirl plays in setting the film length is critical to properly sizing the length of the injector cup for liquid rocket applications

A. Varying Swirl

Figure 3 shows representative instantaneous images of the injector cup for three different injector configurations, 8H-DA-ONPNTN, 8H-ONPNTN, and 4H-ONPNTN, with the same total momentum flux ratio but with varying degrees of swirl; the axial to total velocity ratios are 41, 26, and 30 percent, respectively. In these images the green dashed lines are the instantaneous film profiles, the red marks are the instantaneous film length, and the blue lines are the edge of the injector cup. Flow is left to right. The end of the gas post and the downstream portion of the liquid cup can be seen in the far left of each image. The three cases shown in Fig. 3 look very similar. The film profile is not smooth, but bulges and thins as turbulent gas phase structures interact with the film. Both the top and bottom film length are of similar but slightly different lengths. Most of this difference can be attributed to real structures that corresponded to observed nonuniformities in the spray, but some of this difference is caused by the swirling liquid flow and differences in lighting. A discussion of the difference in average film length between the top and bottom profile was provided in previous work.[2] Throughout this paper, the film length provided is the average of the top and bottom film length. One difference that was observed with varying swirl, but not obvious from Fig. 3, was that entrainment of gas into the liquid film, in the form of bubbles, increased as the radial velocity decreased. This increase in entrained gas corresponds to a decrease in the centripetal force, as would be expected, since the centripetal force acts to stabilize the film.

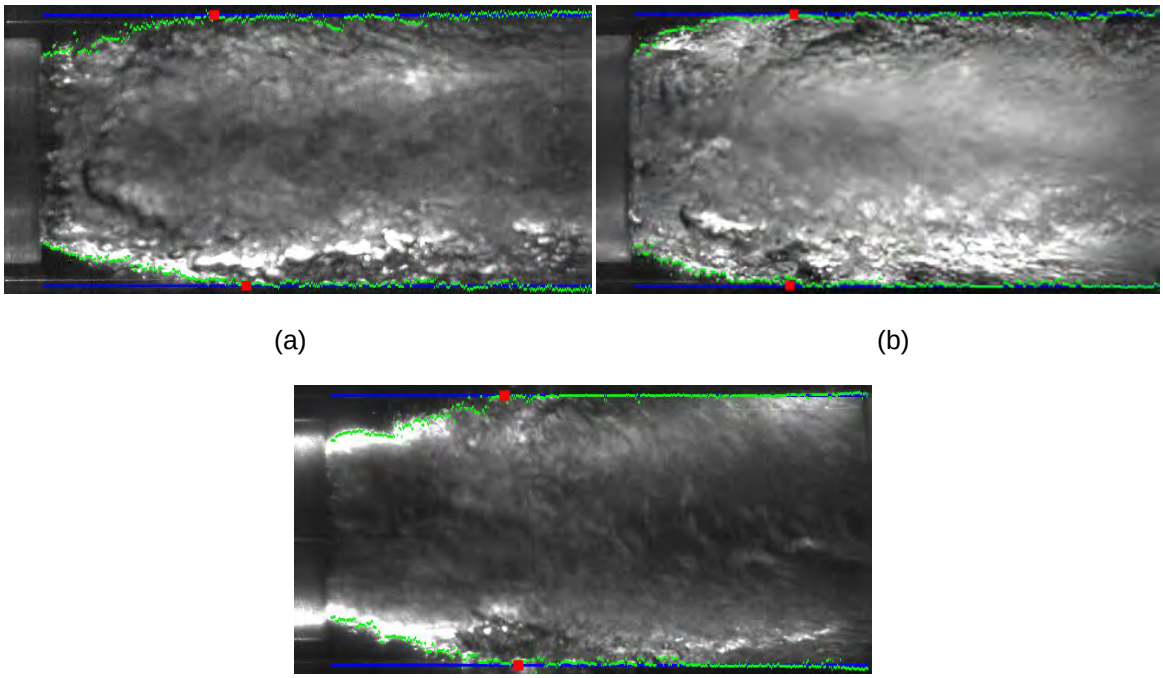

Figure 3. Representative instantaneous injector cup image of the 8H-DA-ONPNTN (a), 8H-ONPNTN (b), and 4H-ONPNTN injector configurations. Momentum flux ratio (Φ_{Total}) is ~71. Blue lines are the boundaries of the injector cup, green lines are the instantaneous film profile and red squares mark the instantaneous film length.

In previous work, Φ_{axial} (Eq. 1) was used to scale the average film length of GCSC injectors, but as discussed earlier, it was unable to collapse all geometries to a single curve making the overall scaling substantially less powerful.[10] Varying insert geometries tended to fall onto a single curve while varying outlet diameters resulted in separate curves. An example of this separation is shown in Fig. 4a. These three cases have both different outlet radius and different cup geometries. Injector dimensions are given in Table 1. Error bars are the standard deviation of the film length. In general the film length behaved as expected: as the momentum of gas phase increases the film atomizes faster resulting in a shorter film up to the point where a minimum length is reached.

In an effort to collapse all geometries to a single curve a different method to calculate the momentum flux ratio- based on calculated gas phase properties and the total liquid velocity vector- was exercised. This method is outlined in Section III. Figure 4b plots normalized film length versus Φ_{total} (Eq. 2) for the same three injector geometries shown in Fig. 4a. Using this new method a reasonable single curve collapse is achieved. Some variation does exist between the three geometries at the higher momentum flux ratio, and it would be easy to assume that this variation is due to an unaccounted for centripetal force. However, the variations seen in Fig. 4b are opposite of what would be expected from stability arguments. R_A for the three geometries used in Fig.4 are very similar- 29, 30, and 32 percent for OUHUTD, ONPNTN, and ODHNTN, respectively. The difference in the centripetal force is mostly driven by the difference in radii 11.4, 9.53, and 7.62, respectively. The pseudoFroude number for centripetal force (Fr_c) can be estimated from Eq. 4 and is only a function of geometry and, therefore, does not vary with the changing momentum flux ratio. Using Eq. 4, values of Fr_c were found to be 0.11, 0.16, and 0.20 for OUHUTD, ONPNTN, and ODHNTN, respectively. Using the idea that centripetal force decreases disturbance size on the surface of the film and therefore hinders atomization one would expect OUHUTD (which has the lowest centripetal force) to have the shortest film length, but the opposite occurs. Either some other unknown mechanism is at work or the centripetal force is working in a manner that is not fully understood.

To further explore the effect of swirl two additional injector bodies were designed with the nominal outlet diameter (19.1 mm), but varying sizes and numbers of the tangential liquid inlet holes. These injector bodies are described in Section II. One of these eight-hole injectors has double the total inlet area (8H-DA-insert) of the nominal (four-hole) case and the other eight-hole injector has the same total inlet area (8H-insert) as the nominal case. The axial to total velocity ratio for these inlet configurations are 30, 41, and 26 percent for 4H-insert, 8H-DA

insert, and 8H-insert, respectively, and are independent of the insert. Figure 5a shows the film length for insert ONPNTN plotted against Φ_{axial}. Despite the fact that the three configurations have the same outlet diameter this definition is unable to collapse the film lengths to a single curve. It does collapse the data into families of curves based on the inlet geometry. Using the momentum flux ratio defined from the total liquid velocity and calculated gas phase density and velocity values (Φ_{total}) the same data can be made to collapses to a single curve as shown in Fig. 5b. At the higher momentum flux ratios the same respectable collapse can be obtained for the other tested inserts, ONPUTN and ONPDTN, as shown in Fig. 5c and d. As shown in Fig. 5c and d, there is a good deal of scatter in the data at the lower momentum flux ratios which is related to previously observed and described nonuniformities in the spray.[10, 12] This increase in the unsteadiness can also be seen in the error bars which, in general, increase in length as momentum flux ratio decreases. The error bars are the standard deviation of the film length and largely consists of the natural film-length fluctuations at those lower ratios. Nonuniformities manifest themselves as spray centerline departures and pulsing phenomenon and have been shown to be caused by complex flow structures such a flow separation and recirculation at the injector-post lip. Given the complexities of these phenomenons it is not surprising that they cause deviations from the momentum flux ratio scaling and cannot be entirely predicted by the momentum flux ratio.

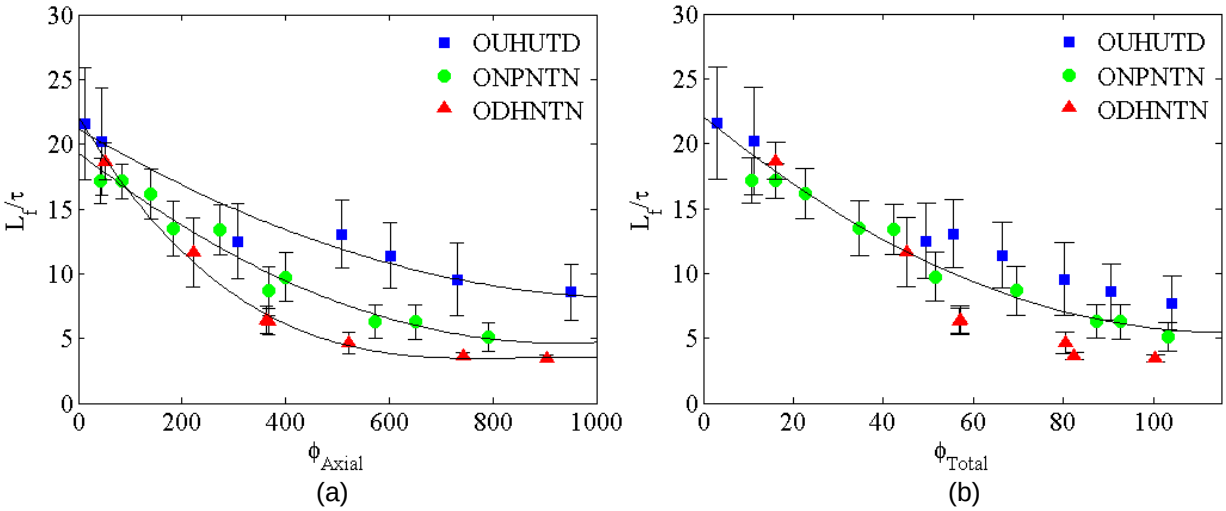

Figure 4. Average film length normalized by the initial film thickness plotted against the momentum flux ratio defined using the axial velocity (a), Eqn. 1, and against the momentum flux ratio using the total velocity and calculated gas phase density and velocity(b), Eqn. 2. Error bars are the standard deviation of the film length.

Figure 6 plots all film lengths from the three injectors and three tested inserts against the momentum flux ratio defined using the total velocity and calculated gas phase density and velocity. At higher momentum flux values the collapse is excellent, but at lower values the spread becomes fairly wide due to the previously discussed nonuniformities. The collapse becomes better if the ONPUTN cases are removed. The thick injector post lip of this insert has been shown to have a rich unsteady behavior. Overall, the momentum flux ratio defined using the total velocity and a calculated gas phase density and velocity value captures the majority of the effect of swirl on the film length.

While the momentum flux ratio, when defined using the total liquid velocity and calculations for the gas phase velocity and density, appears to account for the majority of the effect of swirl on the film length there are phenomenon that are unaccounted for and should be noted. First, centripetal force is completely ignored. Given the similar levels of Fr_c in all of the cases studied here (0.108 to 0.195 using Eq. 4) and the secondary importance of the centripetal force compared to the aerodynamic forces, it is not surprising that no effect of centripetal force is observed. A large deviation in the centripetal force such a going to zero is required to compare the effect and will be discussed in the no swirl section. Second, the loss of momentum in the liquid cup is ignored. Given the inlet liquid velocities (1.3-11.1 m/s) and narrow injector cup, these losses could be significant in calculating the total velocity at the end of the liquid cup. Unfortunately, the complex flow field makes direct calculations unfeasible and the tight enclosed geometry makes direct measurement of the velocity field (while possible) difficult, which leaves costly three-dimensional CFD simulations as the best option. Third, the liquid total velocity vector is used and

directionality of the velocity vector is ignored. Finally, it is assumed that the complex velocity field, which under certain conditions is sonic, can be described using a single velocity value. In entrainment arguments from which momentum flux ratio scaling are typically derived, one or both of the fluid streams is assumed to extend to infinity resulting in a uniform velocity with downstream distance on one side of the mixing layer.[13] In this case, both streams are confined and both streams have an evolving velocity field due to the interaction with the higher momentum gas stream (the liquid film) and the expansion at the injector post lip (the gas stream). Given these limitations, the momentum flux does an excellent job of capturing the film length behavior over a wide range of flow conditions and geometries for GCSC injectors and remains easy enough to calculate in seconds.

In addition to investigating the effect of swirl on liquid film length, the average film profiles were studied to look for variations in the film evolution with changing swirl. Figure 7 shows the average film profile for the three different liquid inlet configurations with the same insert (ONPNTN) at 4 different Φ_{total} values. In general the three configurations follow a similar pattern. At low momentum flux ratio the film persists the majority of the way down the cup and the profile has a small deviation where the slope changes. At higher momentum flux ratios this deviation disappears and the film becomes increasing short. To aid in comparing the film profiles at different swirl levels, the film profiles for the three liquid inlet configurations were plotted together based on Φ_{total}; these are shown in Fig. 8.

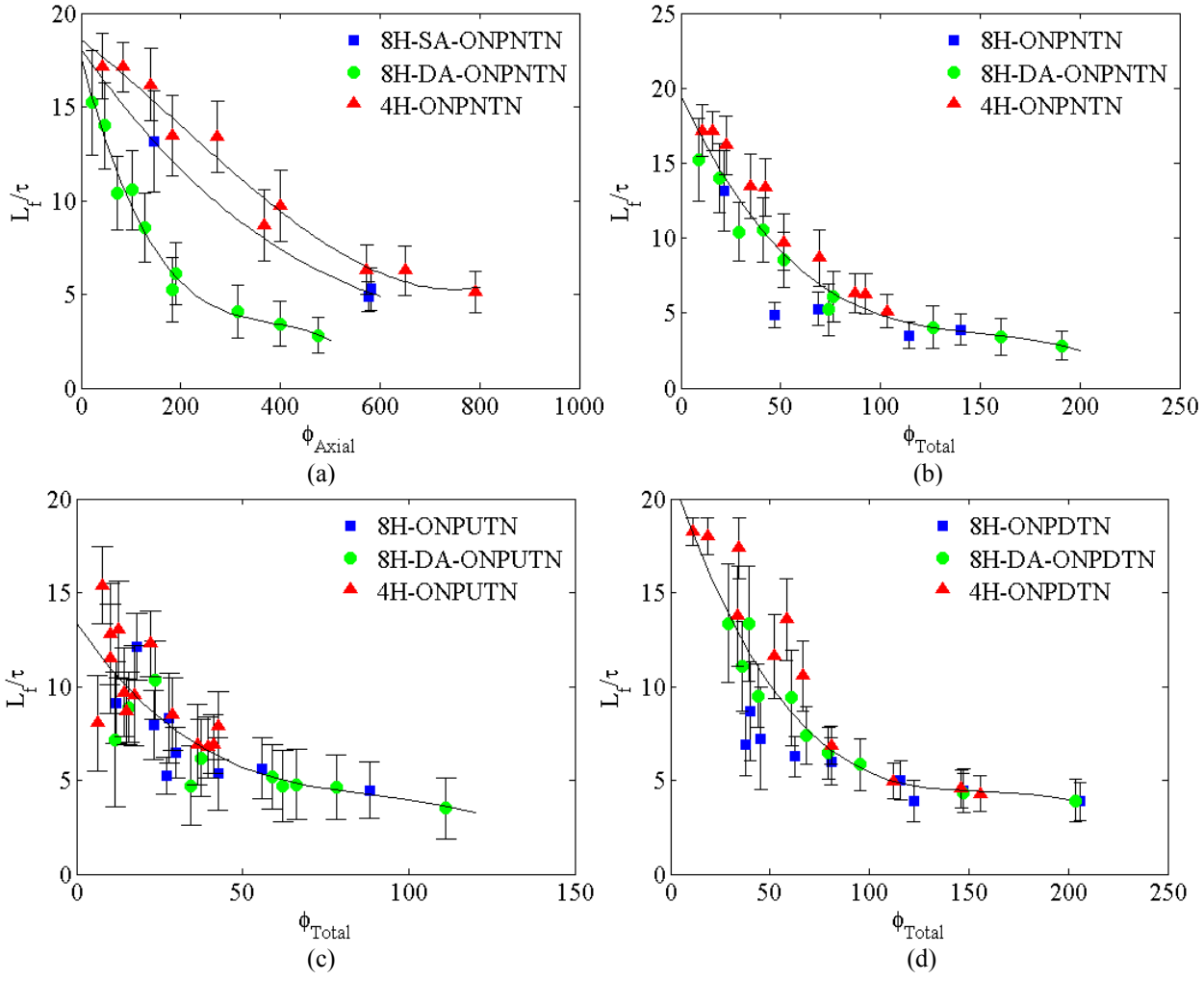

Figure 5. Average film length normalized by the initial film thickness plotted against the momentum flux ratio defined using the axial velocity for insert ONPNTN (a) and against the momentum flux ratio using the total velocity and calculated gas phase density and velocity for inserts ONPNTN (b), ONPUTN (c), and ONPUTN (d) with varying levels of swirl. The axial to total velocity ratio are 30, 41, and 26 percent for 4H-insert, 8H-DA insert, and 4H respectively. Error bars are the standard deviation of the film length.

For the three Φ_{total}, values the collapse of the film profile is excellent for the two eight inlet hole configuration. However, in the three cases were the four liquid inlet hole configuration is compared to the eight hole configuration, the four hole configuration produces a noticeably thicker film. The four inlet film has a similar initial thickness but has less of an initial slope than the eight inlet hole configuration. This difference in film thickness appears to be independent of Φ_{total}. It cannot be related to the swirl and/or the centripetal force since the four hole configuration has an axial to total velocity ratio and a pseudoFroude that falls between the two eight hole configurations. For example, 4H-ONPNTN has a radial to total velocity ratio of 30 percent compared to 26 and 41 percent for 8H-DA-ONPNTN and 8H-ONPNTN respectively. And 4H-ONPNTN has a Fr_c (Eq. 4) of 0.158 compared to 0.145 and 0.162 for 8H-DA-ONPNTN and 8H-ONPNTN respectively. Instead this difference in film profiles must be related to a nonuniform persistence in film velocity related to the initial jet injection.

The finding that the initial jets can persist in the film and even into the spray is not entirely unexpected. In previous work with a different GCSC injector-which has four tangential liquid inlet holes but no sheltered liquid cup- time gated ballistic images showed rotating ligament like structures in the spray that could be traced back to the liquid injection holes.[14] An image of these structures is shown in Fig. 9b. Note that due to multiple scattering light effects these structures cannot be seen by eye or traditional shadowgraphy (Fig 9a). Also, persistence has been documented in diesel sprays.[15] Following this previous work, the sheltered liquid cup was added to the GCSC injector to aid in producing a uniform film before the liquid-gas interaction. Direct images of the liquid cup indicate that the cup fills completely, so any memory of the initial liquid jets must take the form of a nonuniform velocity field. Note that the alignment of the inlet hole and the imaging plane is the same for all configurations. The eight hole configurations' additional inlets are located between the baseline four holes. Additional ballistic images are needed to see if the addition of the injector cup and the additional liquid inlet holes reduces or eliminates the nonuniformities in the spray caused by memory of the liquid injection holes. Time-resolved spray mass distributions obtained using X-ray radiography would show how the liquid injection holes effect the spray mass distribution.

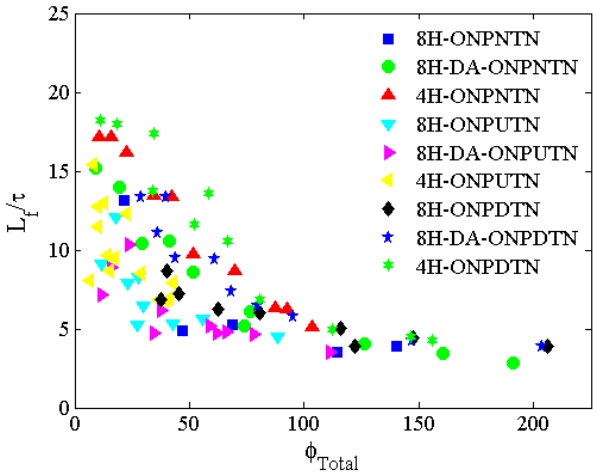

Figure 6. Average film length normalized by the momentum flux ratio using the total velocity and calculated gas phase density and velocity for inserts ONPNTN (b), ONPUTN (c), and ONPUTN (d) with three tangential liquid inlet hole configuration. The axial to total velocity ratio are 30, 41, and 26 percent for 4H-insert, 8H-DA insert, and 4H respectively.

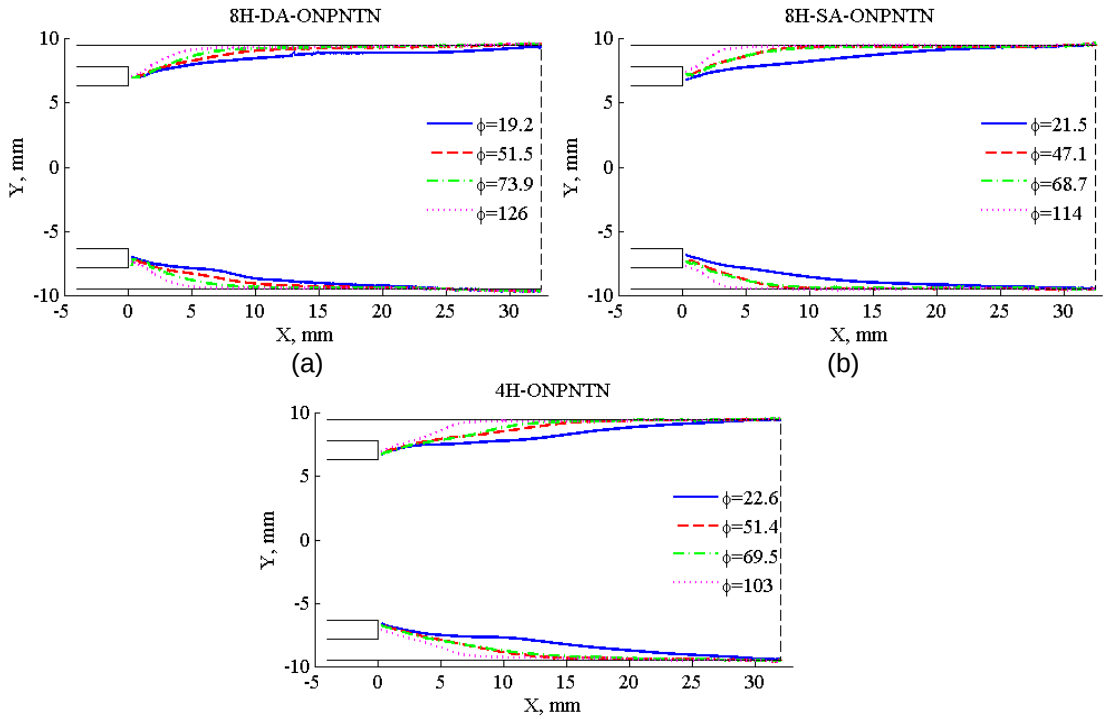

Figure 7. Average film profiles at various momentum flux ratios for three different injector configurations with varying degrees of swirl; 8H-DA-ONPNTN (a), 8H-ONPNTN (b) and 4H-ONPNTN.

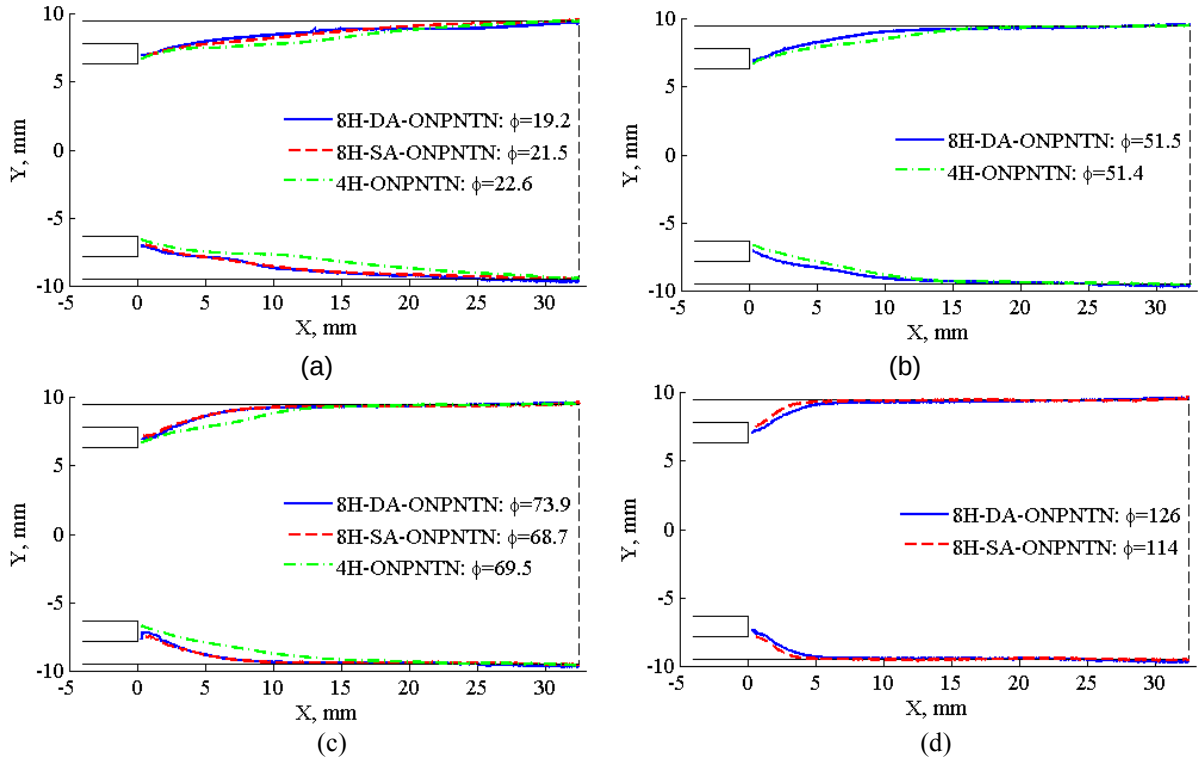

Figure 8. Average film profiles for three different injector configurations with varying degrees of swirl at four momentum flux ratios based on the total liquid velocity; Φ_{total}≈21 (a), Φ_{total}≈51 (b), Φ_{total}≈71 (c), and Φ_{total}≈120 (d).

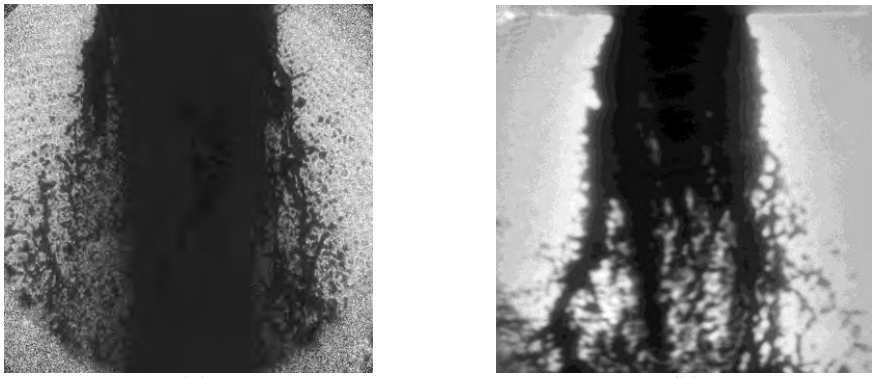

(a) (b)

Figure 9. Shadowgraphy (a) and time-gated ballistic images (b) of a Gas-Centered Swirl-Coaxial injector with four tangential liquid inlet holes and no sheltered liquid cup. Time-gated ballistic image shows film ligaments that can be traced back to the liquid injection holes.

B. No Swirl

An additional method used to investigate the effect of swirl in GCSC injectors was to build an injector without swirl. As discussed in Section II an injector body was build with eight liquid injection holes perpendicular to the liquid cup resulting in a purely axial liquid flow. When processing the images from this no swirl injector (NS-insert) a few problems arose. One, without the swirl the corrugation of the film surface increased resulting in a decrease in amount and uniformity of light scattering towards the camera. This decrease in uniformity made it difficult in some cases for the image processing program to reliably find the film edge; an example of an acceptable film profile is shown in Fig. 10a. Second, as the liquid injection velocity was increased to values comparable to the swirling cases the liquid cup would not completely fill, as shown in Fig. 10b, making it impossible to measure a film length. At these high liquid inlet velocities the liquid jets simply impinged on the far wall of the liquid cup and formed an expanding sheet that did not merge with neighboring sheets leaving room for gas entrainment into the liquid cup. Without the initial uniform film it was not possible to measure a film length nor would it have been a valid comparison with uniformly filled liquid cup cases. In the future, it would be possible to eliminate this problem by increasing the liquid inlet area.

The final problem that arose when processing the nonswirling cases was the increase in the large scale structures on the film surface greatly increasing the entrainment of gas into the liquid film, as shown in Fig. 10c. The increased quantity of bubbles in the liquid film at times made it difficult for the image processing program to find the film edge. An additional reason for the increased bubble entrainment is that the centripetal force created by the swirl creates an artificial gravity in the film which results in a buoyancy force acting on the bubbles in the swirling case. This buoyancy force hinders entrainment and decreases the distance entrained bubbles can penetrate the film. These issues greatly decreased the number of cases that reliably could be compared to their swirling counterparts.

Normalized film length versus Φ_{total} is plotted in Fig. 11 for three inserts and all four liquid inlet hole configurations. For the nonswirling, cases the momentum flux ratio is calculated using the axial liquid velocity assuming the liquid cup is uniformity filled. Conservation of momentum is not used. For all insert geometries at the lower momentum flux ratios (less than 50) the no swirl cases fall below the swirling cases. Since the centripetal acceleration acts as a stabilizing force in the swirl cases, it is not surprising that eliminating the swirl decreases the film length. Also the lower the momentum flux ratio the less dominate the aerodynamic forces resulting in a greater role played by the centripetal force. As the momentum flux ratio, is increased the aerodynamic forces should again become dominate and the centripetal acceleration will play less of a role. Unfortunately, due to the previously discussed issues only one point with a momentum greater than 50 is shown in Fig. 11a. While inconclusive, it does show as Φ_{total} increases the nonswirling and swirling cases approach the same minimal film length.

Given the shortness of the nonswirling cases it might be tempting to ask why the liquid film is swirled at all. When using a GCSC injector as a propellant injector in a liquid rocket engine having the shortest possible film is not necessary desirable even though a shorter film could mean a shorter and, therefore, a lighter injector. If the film is too short, the injector might not be sufficiently cooled which could result in melting of injector faceplate resulting in damage to the engine. Also, these nonswirling short films are very unsteady with large deviation height and length which produce unsteadiness in the spray. When designing a GCSC injector for an engine application stability,

injector performance, mixture ratio, injector life and throttleability concerns must be balanced when deciding on the appropriate amount of swirl and the injector cup length. It remains for later work to look at the relative stability of the spray and uniformity of the mass distribution with varying levels of swirl and inlet hole configuration.

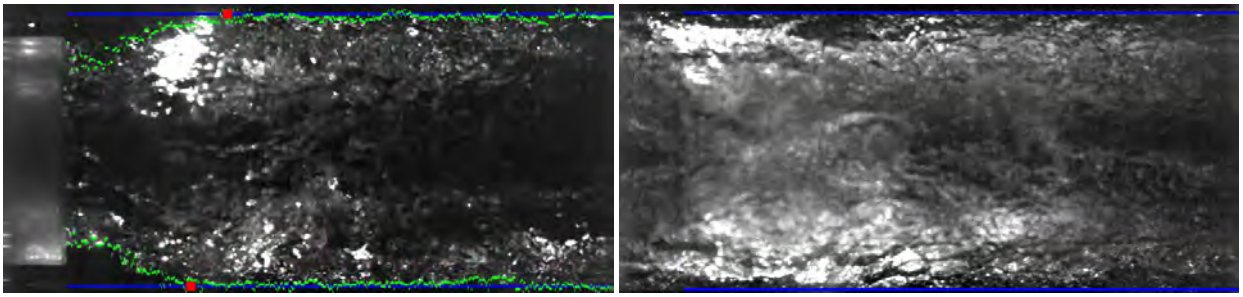

(a) (b)

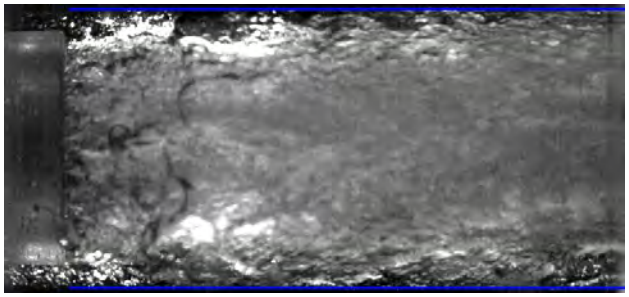

(c)

Figure 10. Representative instantaneous injector cup images of the NS-ONPNTN injector configuration. Subfigures show a measurable film length case (a), an unfiled liquid cup case (b), and a case with upstream bubble entrainment (c). Blue lines are the boundaries of the injector cup, green lines are the instantaneous film profile and red squares mark the instantaneous film length.

V. Conclusion

An updated definition of the momentum flux ratio has been presented. Instead of an overly simplistic treatment based on atmospheric properties and measured mass flow rates, the new definition uses one-dimensional gas dynamics to calculate gas velocity and density from the measured mass flow rate, total temperature and static pressure. The liquid velocity used is now the total velocity as opposed to the axial velocity. Total velocity is calculated from a combination of mass flow rate and momentum conservation from the liquid inlet to the end of the sheltering step (i.e., just prior to where the gas and liquid meet). This definition collapses the data over a range of conditions, including a range of liquid swirl levels. Changes in injector outlet diameter, liquid inlet velocity, and the geometry near liquid-gas contact were investigated and the momentum flux ratio does a good job of scaling the liquid film length. Over the range of geometries, the film length data collapses onto a single curve versus Φ_{total}.

The amount of swirl and, associated with that, the pseudoFroude number for centripetal force does not impact the length of the film. As a result, changes in the outlet diameter of the injector and the inlet geometry do not impact the momentum flux ratio scaling. When the value of the centripetal force parameter is compared to the momentum flux ratio, this outcome is expected, as the two differ by several orders of magnitude. However, when the swirl goes to zero and the momentum flux ratio is under 50, the measured film length is shorter than any of the cases with swirl. As the momentum flux ratio increases, the values come together. While likely related to the stabilizing effect of swirl, this finding may be indicative of its effect on the gas-phase recirculation following the lip separating the gas and liquid as much as the swirl's stabilizing of the liquid.

Despite little effect on film length, the swirl cannot be completely neglected: it does alter the character of the film. At higher axial to total velocity ratios (i.e., lower swirl numbers), the amount of air entrained into the film

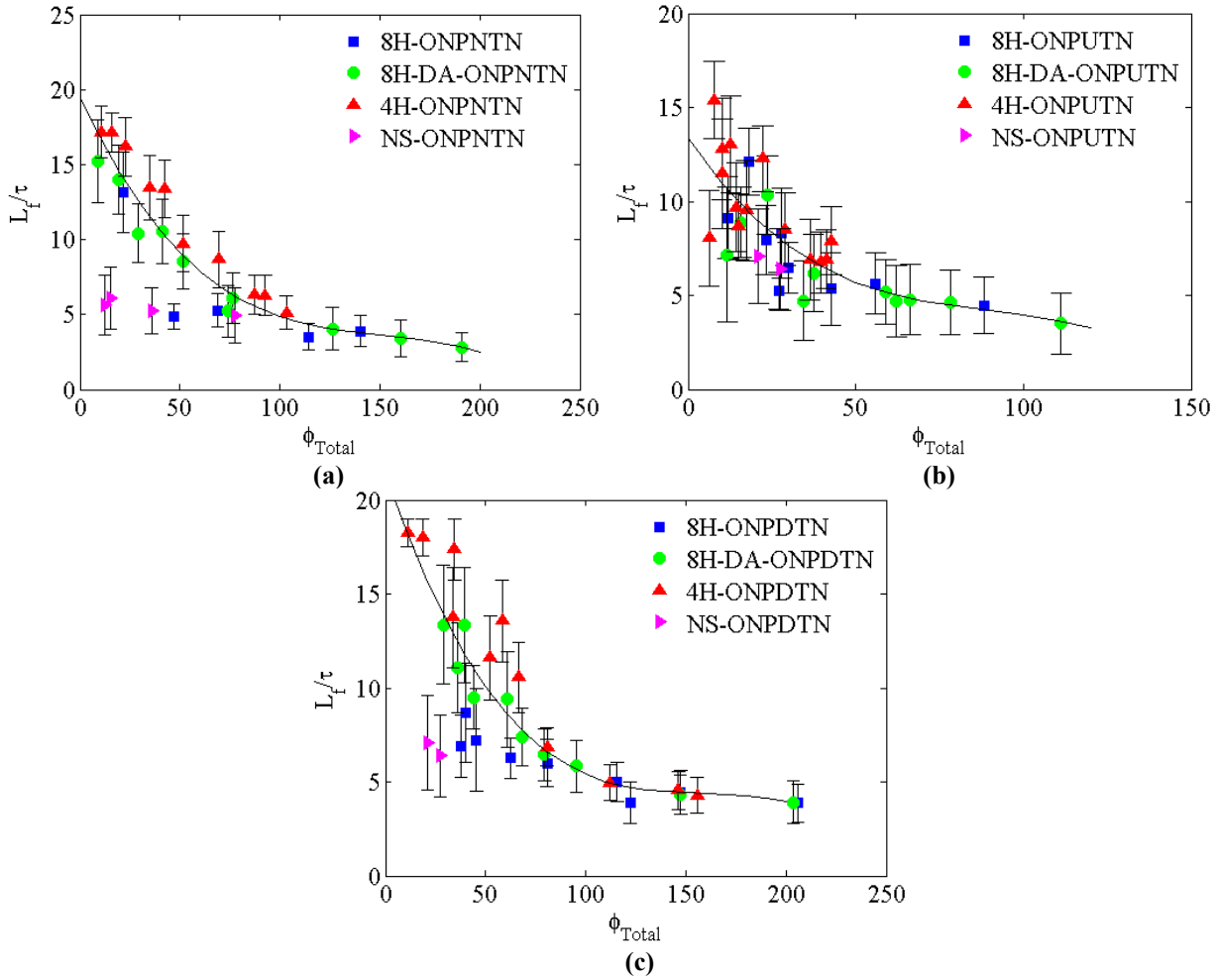

Figure 11. Average film length normalized by the initial film thickness plotted against the momentum flux ratio using the total velocity and calculated gas phase density and velocity for inserts ONPNTN (b), ONPUTN (c), and ONPUTN (d) with varying levels of swirl. The axial to total velocity ratio are 30, 41, 26, and 0 percent for 4H-insert, 8H-DA-insert, 4H-insert, and NS-insert respectively. Error bars are the standard deviation of the film length.

increases. When the swirl goes to zero, the amount of gas entrained can make automated boundary finding impossible. The zero swirl tests also have greatly increased unsteadiness, especially in film height. Because unsteadiness in the film generally translates into unsteadiness in the spray, the zero swirl findings suggest that some swirl is desirable to improve engine performance. Difficulties in always forming a liquid sheet when there was no swirl also emphasizes the need for swirl to help produce uniform sprays.

Initially, it appeared that the swirl had an impact the film thickness as well. Close inspection of the data, however, shows that the minimal and maximal swirl cases—which both have 8 inlet holes—have similar thicknesses while the central value—which has 4 inlet holes—is thicker. Instead of being related to swirl, then, these changes in thickness appear to be related to the inlet geometry. This implies that momentum is remaining discrete within the liquid sheet, so that, while individual liquid jets are not visible in the cup the film is, to an extent, behaving as if it were individual jets. Downstream of the cup, observations further supporting this finding have been reported using a similar type of injector.

Overall, then, it is recommended that the momentum flux ratio based on total liquid velocity and a gas velocity and density based on one-dimension compressible flow be used to scale the intact film length and, ultimately, the atomization rate and efficiency. This scaling is appropriate over a range of finite swirl conditions and, even with zero swirl, at ratios over 50. To produce uniform and more stable sprays, some level of swirl is recommended in the

design of GCSC injectors. Again, at operations above momentum flux ratios of 50 the swirl will not impact the atomization efficiency but it will improve the spray quality.

References

[1]Lightfoot, M.D.A., S.A. Danczyk, and D.G. Talley. "Atomization in Gas-Centered Swirl-Caxial Injectors," *19th ILASS Americas,* Toronto, Canada, 2006.

[2]Schumaker, S.A., S.A. Danczyk, and M.D.A. Lightfoot. "Effect of Cup Length on Film Profiles in gas-Centered Swirl-Coaxial Injectors," *48th AIAA Aerospace Sciences Meeting,* 2010-368, Orlando, Fl, 2010.

[3]Canino, V.J., et al. "Unsteady Respinse of Recessed-Post Coaxial Injectors," *41st AIAA Joint Propuslion Conference,* AIAA 2055-4297, Tucson Arizona, 2005.

[4]Fu, Q.-f., L.-j. Yang, and Y.-y. Qu, "Measurement of annular liquid film thickness in an open-end swirl injector," *Aerospace Science and Technology*, Vol. 15, No. 2, 2011, pp. 117-124.

[5]Im, J.H., S. Cho, and Y. Yoon, "Comparative Study of Spray Characteristics of Gas-Centered and Liquid-Centered Swirl Coaxial Injectors," *Journal of Propulsion and Power*, Vol. 26, No. 6, 2010, pp. 1196-1204.

[6]Kulkarni, V., et al., "Liquid Sheet Breakup in Gas-Centered Swirl Coaxial Atomizers," *Journal of Fluid Engineering*, Vol. 132, No. 1, 2010.

[7]Dranovsky, M.L., "Combustion Instabilities in Liquid Rocket Engines: Testing and Development Practices in Russia," *Progress in Astronautics and Aeronautics*, Vol. 221, No. 2007.

[8]Lightfoot, M.D.A., S.A. Danczyk, and D.G. Talley. "A Method to Predict Atomizer Performance in Gas-Centered Swirl-Coaxial Injectors " *2007 ILASS-Americas,* Chicago, IL 2007.

[9]Strakey, P., R.K. Cohn, and D.G. Talley. "The Development of a Methodology to Scale between Cold-Flow and Hot-Fire Evaluations of Gas-Centered Swirl Coaxial Injectors," *17th ILASS Americas,* Arlington, VA, 2004.

[10]Lightfoot, M.D.A., S.A. Danczyk, and D.G. Talley. "Scaling of Gas-Centered Swirl-Coaxial Injectors," *JANNAF 6th Modeling and Simulation/ 4th Liquid Propulsion/ 3rd Spacecraft Propulsion Joint Subcommitte Meeting,* Orlando, FL, 2008.

[11]Lightfoot, M.D.A., "Fundamental Classification of Atomization Processes," *Atomization and Sprays*, Vol. 19, No. 11, 2009, pp. 1065-1104.

[12]Lightfoot, M.D.A. and S.A. Danczyk. "Spray Nonuniformities in Gas-Centered Swirl-Coaxial Injectors," *11th Triennial International Conference on Liquid Atomization and Spray Systems,* Vail, CO, 2009.

[13]Brown, G.L. and A. Roshko, "On Density Effects and Large Structure in Turbulent Moxing Layers," *Journal of Fluid Mechanics*, Vol. 64, No. 1974, pp. 775-816.

[14]Schmidt, J.B., et al., "UIltrafast Time-Gated Ballistic-Photon Imaging and Shadowgraphy in Optically Dense Rocket Sprays," *Applied Optics*, Vol. 48, No. 4, 2009, pp. 137-144.

[15]Soteriou, C., et al. "Through the Diesel Nozzle Hole-- a Journey of Discovery," *14th ILASS,* Dearborn, MI, 2001.